

Thermonuclear supernova models, and observations of Type Ia supernovae

E. Bravo^{*†}, C. Badenes^{**} and D. García-Senz^{*†}

^{*}*Dept. Física i Enginyeria Nuclear, UPC, Av. Diagonal 647, 08028 Barcelona*

[†]*Institut d'Estudis Espacials de Catalunya, Barcelona*

^{**}*Dept. Physics and Astronomy, Rutgers Univ., 136 Frelinghuysen Rd., Piscataway NJ 08854-8019*

Abstract. In this paper, we review the present state of theoretical models of thermonuclear supernovae, and compare their predictions with the constraints derived from observations of Type Ia supernovae. The diversity of explosion mechanisms usually found in one-dimensional simulations is a direct consequence of the impossibility to resolve the flame structure under the assumption of spherical symmetry. Spherically symmetric models have been successful in explaining many of the observational features of Type Ia supernovae, but they rely on two kinds of empirical models: one that describes the behaviour of the flame on the scales unresolved by the code, and another that takes account of the evolution of the flame shape. In contrast, three-dimensional simulations are able to compute the flame shape in a self-consistent way, but they still need a model for the propagation of the flame in the scales unresolved by the code. Furthermore, in three dimensions the number of degrees of freedom of the initial configuration of the white dwarf at runaway is much larger than in one dimension. Recent simulations have shown that the sensitivity of the explosion output to the initial conditions can be extremely large. New paradigms of thermonuclear supernovae have emerged from this situation, as the Pulsating Reverse Detonation. The resolution of all these issues must rely on the predictions of observational properties of the models, and their comparison with current Type Ia supernova data, including X-ray spectra of Type Ia supernova remnants.

INTRODUCTION

The huge increase in number, quality and diversity of observational data related to Type Ia supernovae (SNIa) in recent years, combined with the advance in computer technology, have persuaded modellers to leave the phenomenological calculations that rely on spherical symmetry, and attempt more physically meaningful three-dimensional (3D) simulations. Although the more plausible models of the explosion always involve the thermonuclear disruption of a white dwarf [1], the current zoo of explosion mechanisms is still too large to be useful in cosmological applications of Type Ia supernovae or to make it possible to understand the details of the chemical evolution of the Galaxy. Nowadays, the favoured SNIa model is the explosion of a white dwarf that approaches the Chandrasekhar-mass limit owing to accretion from a companion star at the appropriate rate to avoid the nova instability [2, 3]. Going beyond this general picture into the details of the supernova explosion is not easy, especially with respect to the multidimensional models that are just beginning to appear in the literature. In particular, the prediction of the optical light curve or spectra of a 3D model is still out of reach, and therefore it is necessary to rely on other gross features of the observations in order to estimate the viability of a given model.

The most relevant property of SNIa is the homogeneity of their light curve and spectral evolution. The light curve is powered by the radioactive decay of ^{56}Ni and ^{56}Co [4], but the range of nickel masses allowed by the observations varies by about a factor five from low-luminosity SNIa up to normal events. Although the shape of the light curves can be described by a one-parameter relationship between brightness and width of the curve [5, 6, 7, 8], due to the dependence of opacity on temperature, there still remains a residual scatter of ~ 0.2 mag around the template curves. The main spectral features of normal (bright) SNIa at early photospheric phase include the absence of conspicuous lines of H and the presence of strong SiII absorption lines together with absorption lines of other intermediate mass elements (CaII, SII, OI) spanning a range of velocities from 8,000 up to 30,000 km s^{-1} . The nebular phase is dominated by Fe lines. Usually, the spectral evolution is attributed to the recession (in terms of lagrangian mass) of the photosphere through a layered chemical structure. Recent spectroscopic observations of a dozen *Branch-normal* Type Ia supernovae in the near infrared [9] suggest that the unburnt matter ejected has to be less than 10% of the mass of the progenitor. According to these results, the presence of a substantial amount of unburnt low-velocity carbon near the center of the star is rather improbable.

A relevant question for multidimensional simulations, is whether there is any significant observational evidence of departure from spherical symmetry in the SNIa sample. In this regard, there are several signs that the departure from spherical symmetry is not large: the low level of polarization of most SNIa, although there are exceptions [see, for instance, 10], the homogeneity of the profile of the absorption line of SiII [11], and the fact that galactic and extra-galactic young Type Ia supernova remnants (SNR) do not show large departures from spherical symmetry.

The spectral homogeneity of normal SNIa near maximum brightness is particularly relevant for the discussion below. By comparing the spectra of four normal SNIa (SN 1989B, SN 1990N, SN 1994D, and SN 1998bu) Thomas et al. [11] have shown that the absorption features of SiII displayed quite homogeneous profiles from event to event. Such homogeneity can be used to constrain the presence of chemically inhomogeneous clumps at the photosphere, through the effect they would have on the line profiles. Specifically, Thomas et al. [11] limited the size of the clumps to be less than $\sim 30\%$ of the radius of the photosphere.

To summarize the gross constraints imposed by SNIa observations, the *overall* shape of the supernova has to be spherical (low polarization), there are not large chemically inhomogeneous blobs at the photosphere at maximum light (homogeneous SiII line profiles), and the chemical composition of the ejecta has to retain a high degree of stratification. One has to keep in mind that subluminous as well as superluminous events display a peculiar spectral evolution. For the time being, however, as long as multidimensional simulations are concerned, the main objective is to explain the gross properties of normal SNIa. In the first part of this paper, we will review the results of recent 3D simulations of thermonuclear supernovae (TSN), and compare their predictions with observational data. In the second part, we will discuss the prospects for the use of X-ray spectra of supernova remnants to discriminate between the different explosion mechanisms or progenitor scenarios that are currently advocated to explain SNIa.

3D MODELS OF THERMONUCLEAR SUPERNOVAE

From a theoretical point of view, there remain several fundamental issues to be solved:

- What is the progenitor system and how does the white dwarf manage to reach the Chandrasekhar mass?
- What is the evolution of the white dwarf short before carbon runaway? and how, when, and where does the ignition process begin?
- How does the flame propagate through the white dwarf once ignited?
- Is a deflagration-to-detonation transition possible, and under which conditions?
- What is the role played by the rotation of the white dwarf?

Here, we will not discuss the presupernova evolution, which is addressed at length in other contributions to this volume. However, it is worth to remark that the output of the explosion in terms of its kinetic energy, density profile, and chemical composition is determined in the first few seconds after runaway, and is not much sensitive to the details of the presupernova evolution. The only features of the progenitor system that influence the explosion are the C/O ratio and metallicity of the white dwarf, its central density (determined by the accretion rate), and rotation (see the contributions by Piersanti et al. and Domínguez et al. in this volume). However, the supernova properties can be influenced on longer timescales by several characteristics of the progenitor system, owing to the interaction of the ejecta with the secondary star (this is probably the case for the peculiar supernovae SN2000cx and SN2002cx, see e.g. Thomas et al. [12], Li et al. [13]), with a circumstellar medium (normal Type Ia SN2003du and SN2002ic, see Gerardy et al. [14], Hamuy et al. [15]), or during the formation of the supernova remnant [16].

Spherically symmetric models and early two and three-dimensional calculations of TSN assumed that the ignition started in a central volume. This view was challenged by Garcia-Senz and Woosley [17], who showed that burning blobs formed during the convective preignition phase would be able to float and accelerate up to $\sim 100 \text{ km s}^{-1}$, with the result that the flame would be rapidly scattered in a region 100 – 250 km away from the center of the star. In this case, the flame would not begin just in a central volume but distributed in an exponentially increasing [18, 19] number of hot spots, whose velocity could reach $\sim 1\%$ of the sound velocity.

In order to simulate TSN it is always necessary to approximate the behavior of the flame below the scales not resolved by the hydrocode with a suitable model. This is not an easy task, due to the quite different regimes of thermonuclear flames at high densities, $\rho \sim 10^9 \text{ g cm}^{-3}$, (thin flame of width $< 1 \text{ cm}$, propagating with a low velocity of order 1 – 3% of the sound velocity, and with a surface progressively corrugated by hydrodynamic instabilities on timescales of a few tenths of a second) and at the end of the explosion, $\rho < \text{a few } \times 10^7 \text{ g cm}^{-3}$, (thick flame of width similar to the white dwarf radius, subject to mixing between ashes and fuel *before* completion of the nuclear reactions, which favours the production of intermediate mass elements). The range of involved lengthscales spans ~ 9 orders of magnitude, which on one hand discards its direct resolution with any hydrodynamical code but, on the other hand, allows to use a statistical description of the flame. Up to now, there is no convergence between the

different approximations adopted by different 3D hydrocodes.

Deflagrations and delayed detonations

The multidimensional calculations of deflagrations carried out so far [see 20, 21, 19, for the most recent results] have shown interesting deviations from what is predicted in spherically symmetric models:

1. The geometry of the burning front is no longer spherical owing to the important role played by buoyancy and hydrodynamic instabilities,
2. the chemical stratification of the ejecta is lost,
3. the amount of ^{56}Ni is sufficient to power the light curve, but it is localized in clumps distributed all along the radius of the white dwarf, and
4. an uncomfortably large amount of carbon and oxygen remains unburnt at the center of the white dwarf.

Three-dimensional simulations have also demonstrated that the flame evolves in quite a different way when calculated in 2D or 3D, due to the different degrees of freedom of the flow. Thus, earlier results of 2D models of thermonuclear supernovae have to be regarded with caution.

The results of the most up-to-date 3D simulations of deflagration supernovae (kinetic energy, K , and masses of ^{56}Ni , M_{56} , intermediate mass elements, M_{ime} , and unburned C+O, M_{CO}) are shown in Table 1. The results obtained under quite different initial conditions and using very different numerical techniques (PPM vs SPH, with degrees of spatial resolution varying by a factor ten, with different subgrid-scale models of the flame, etc) are remarkably homogeneous. The kinetic energy and the amount of ^{56}Ni are compatible with SNIa, but the amount of intermediate mass elements is rather low and the mass of C+O ejected in the explosion is too large, probably by a factor five or more. The convergence of the results obtained with different codes reflects the fact that the main trends of deflagration supernovae are well understood and incorporated into the calculations. There is little hope that further refinements in the methods used to simulate them will substantially change the outcome of current 3D deflagration models.

In the left panel of Fig. 1 it is shown the distribution of ^{56}Ni at the photosphere for the model starting from 30 bubbles of the same size [19]. The size of the clumps is too large to be compatible with the observational limits posed by the homogeneity of the spectral features of SNIa [11]. It is important to keep in mind that the main properties of 3D deflagrations are model independent, as they result from first principles. In particular, the deformation of the flame front due to hydrodynamical instabilities is unavoidable, because the timescale for developing the Rayleigh-Taylor instability is only a few tenths of a second, i.e. about a factor five lower than the time needed by the deflagration to reach the white dwarf surface. Once the spherical symmetry of the flame is lost it is quite difficult to restore it unless a very energetic and impulsive phenomenon, like a detonation, is invoked.

In spite of the success achieved by one-dimensional delayed detonation TSN models, the physical mechanism responsible for the transition from the deflagration to a detona-

TABLE 1. Results of 3D simulations of thermonuclear supernovae

Model	K (10^{51} erg)	M_{56} (M_{\odot})	M_{ime} (M_{\odot})	M_{CO} (M_{\odot})
Deflagrations				
Central ignition with strong turbulence[21]	0.6	~ 0.5	~ 0.1	~ 0.7
Central ignition with realistic turbulence[21]	0.37			
Central ignition[20]	0.48	0.30	0.10	0.75
Ignition in 40 bubbles, large resolution[20]	0.45	0.33	0.23	0.64
Ignition in 30 bubbles of the same size[19]	0.43	0.43	0.07	0.67
Ignition in 90 bubbles of different sizes[19]	0.45	0.44	0.08	0.66
Ignition in 240 bubbles, very large resolution[22]	0.6	0.42	0.10	0.62
Delayed detonations				
Macroscopic transition to detonation[23]	0.75	0.54	0.16	0.34
Local transition in the central region[23]	0.48	0.43	0.10	0.48
Local transition at intermediate radius[23]	0.51	0.42	0.14	0.45
Local transition in the outer layers[23]	0.33	0.34	0.09	0.57
Transition in a central volume[24]	0.8	0.78*		
Off-center transition[24]	0.8	0.73		
Transition in a central volume at high density[24]	1.1	0.94		

* In this and the following models M_{56} represents the approximate yield of Fe-group nuclei

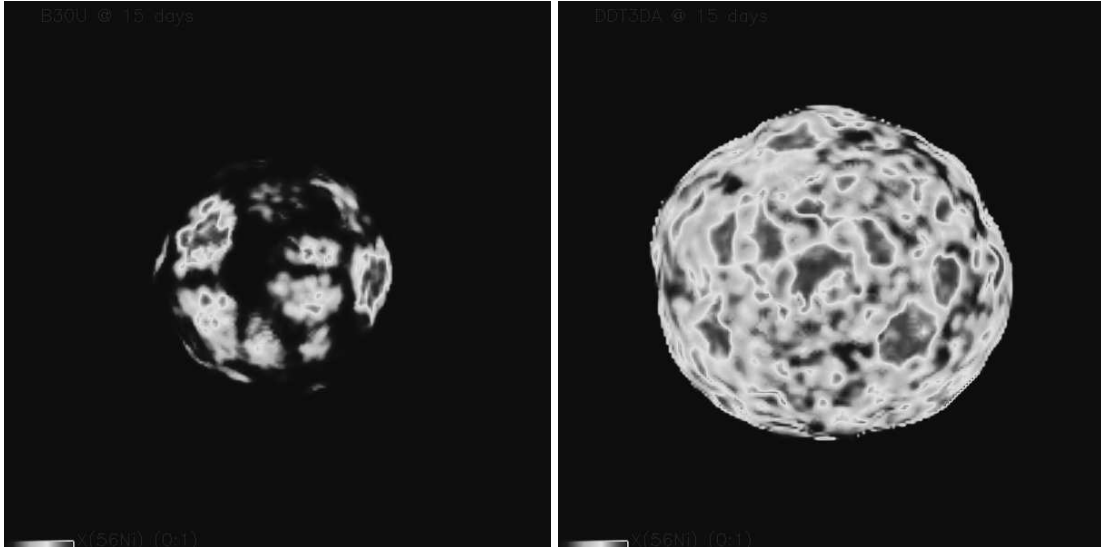


FIGURE 1. Mass fraction of ^{56}Ni at the photosphere 15 days after the explosion. *Left:* Deflagration model. *Right:* Delayed detonation model

tion at the convenient densities ($\sim 10^7 \text{ g cm}^{-3}$) is still unknown. Up to now two different scenarios have been proposed :

- A local transition, induced when a fluid element burns with a supersonic phase velocity when the flame changes from the laminar to the distributed regime [25].

- A macroscopic transition, triggered by a complex topology of the flame that results in a fuel consumption rate larger than that obtained in a supersonic spherical front [26].

The first mechanism has been studied by Lisewski et al. [27] who found that the required mass of the detonator was too large, precluding the formation of a detonation at the densities of interest. The viability of the second mechanism has not been demonstrated so far. Therefore, delayed detonation calculations in 3D are constrained by the uncertainty about the transition density, assuming there is any transition at all. In Table 1 we show the results of the few 3D models of delayed detonation that have been computed up to now. The results obtained by different groups show a larger discrepancy than those derived from pure 3D deflagration simulations. The kinetic energy and the masses of ^{56}Ni and intermediate mass elements are, in general, larger than in 3D deflagration models. Nevertheless, the amount of unburned C-O ejected in the models computed by Garcia-Senz and Bravo [23] is still quite large. In contrast to this situation, the delayed detonation models computed by Gamezo et al. [24] showed that there was no fuel left at the center after the passage of the detonation front. The reason for this apparent discrepancy is the large density of the transition ($> 10^8 \text{ g cm}^{-3}$) adopted by these authors. Both groups also obtained different results with respect to the stratification of the chemical composition in the ejecta.

The clumps formed during the deflagration phase are destroyed by the detonation waves. The distribution of ^{56}Ni resulting for the macroscopic transition delayed detonation model of Garcia-Senz and Bravo [23] (see Table 1) is shown in the right panel of Fig. 1. There, it can be seen how the size of the individual clumps is smaller than in the deflagration case, making 3D delayed detonations compatible with the spectral homogeneity of SNIa.

New explosion paradigms

Although most of the *mildly successful* 3D deflagration models calculated so far start from a large number of bubbles scattered through the central region of a white dwarf, nowadays it is not clear how many hot spots can be present at runaway. Thus, it is interesting to ask what would be the outcome of the explosion if the initial number of bubbles were small? At first sight, one can expect that the energetics of the explosion would be smaller than in the many bubbles models, probably giving rise to a failed explosion and a pulsation of the white dwarf. In this way, the uncertainty about the initial configuration of the flame has allowed the introduction of two new paradigms of TSN, the so-called Pulsating Reverse Detonation (PRD) and the Gravitationally Confined Detonation (GCD).

The PRD mechanism of explosion is a byproduct of the simulations of deflagrations carried out by Garcia-Senz and Bravo [19] starting from 6-7 bubbles. In these simulations, the nuclear energy generated during the deflagration phase was insufficient to unbind the star, as expected. Due to the ability of hot bubbles to float to large radii in 3D models, most of the thermal and kinetic energy resided in the outer parts of the structure, which resulted in an early stabilization of the central region (mostly made of cold C and

O, i.e. fuel) while the outer layers were still in expansion. A few seconds later, an accretion shock formed at the border of the central nearly hydrostatic core (whose mass was about $0.9 M_{\odot}$). As a consequence, the temperature at the border of the core increased to more than 2×10^9 K, on a material composed mainly by fuel but with a non-negligible amount of hot ashes, thus giving rise to a highly explosive scenario. If a detonation were ignited at this point, it would probably propagate all the way inwards through the core, burning most of it and producing an energetic explosion, with a stratified composition. A one-dimensional follow-up calculation of the detonation stage produced a kinetic energy of 0.89×10^{51} erg and $0.35 M_{\odot}$ of ^{56}Ni . At the same time, the amount of unburned C-O was reduced to $0.22 M_{\odot}$.

The GCD mechanism of explosion of Plewa et al. [28] keeps some similarity with the PRD, but this time the runaway starts in a single hot bubble located close to the center of the white dwarf. Once again, the evolution is dominated by the bubble motion towards the surface, which hinders a substantial propagation of the deflagration front and determines the explosion failure. However, it is just following this failure of the deflagration, and the subsequent breakout of the bubble at the surface of the white dwarf, when the most interesting events take place. The bubble material is then spreaded around the surface, where it experiences a strong lateral acceleration while remaining gravitationally confined to the white dwarf. Finally, the material focuses at the pole opposite to the point of breakout, providing a high compression and attaining a high temperature ($> 2.2 \times 10^9$ K). The calculations of Plewa et al. [28] end at this point, but they claim that a detonation will probably form at the point of maximum temperature, propagating through the remaining of the white dwarf and burning it to Fe-group and intermediate mass elements. It has to be noted that this model was the result of a 2D calculation, and its results have still to be confirmed by full 3D simulations.

NEW WINDOWS TO SNIA: THE SN-SNR CONNECTION

The X-ray spectra of supernova remnants originated by SNIa contain important information regarding the physical mechanism behind the explosions. In the process of formation of the remnant, the supernova ejecta interact with the ambient medium surrounding the supernova progenitor, transfer mechanical energy to it, and are heated through shock waves to a state in which both the ambient medium and the ejecta emit X-rays. During the initial phase of the remnant evolution, when the SNR is still young, the emission in the high energy band is determined mainly by the properties of the ejecta. In general, the X-ray emission can have several components:

- A non-thermal continuum, related to the ambient magnetic field, non-maxwellian populations, etc.,
- a thermal continuum (bremsstrahlung), sensitive to the local state of the plasma, and
- thermal line emission, sensitive to the chemical abundances, ionization state, and thermal state of the plasma.

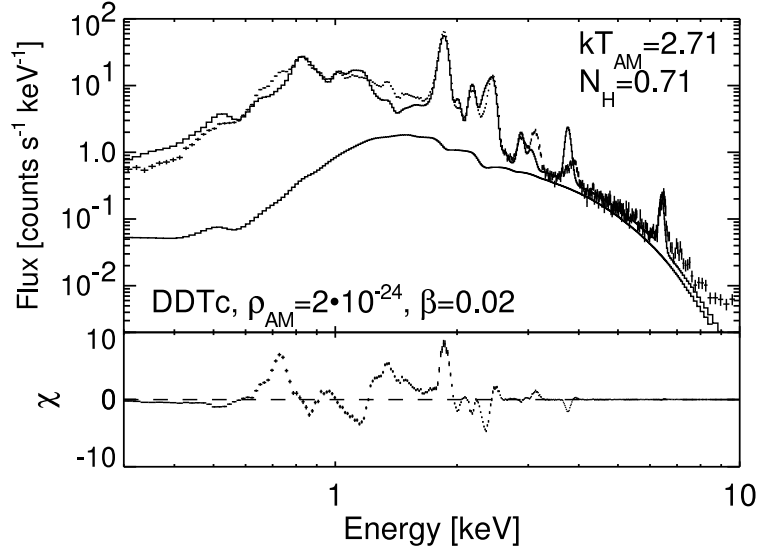


FIGURE 2. The best fit to the *XMM-Newton* spectrum of the Tycho SNR (solid line) is compared to the data (points). The spectrum emitted by the shocked interstellar medium is also shown (featureless solid curve). See Badenes [16] for details

The X-ray line emission from young SNRs provides a convenient way to constrain the nucleosynthetic production and energetic properties of the explosion.

In a recent work, Badenes et al. [29] showed that the differences in chemical composition and density profile of SNIa ejecta have indeed a deep impact on the thermal X-ray spectra emitted by young SNRs. Thus, it is possible to use the excellent X-ray spectra of Type Ia SNRs obtained by X-ray observatories, like *XMM-Newton* and *Chandra*, to constrain Type Ia SN explosion models. Similar approaches were taken in the past by Dwarkadas and Chevalier [30] and Itoh et al. [31], although these works either did not include spectral calculations or were limited to the study of a particular model (the W7 model). Kosenko et al. [32] have undertaken a similar enterprise, whose results are just beginning to appear in the literature. More recently, Badenes [16] has compared the spectra predicted by more than 400 supernova remnant models (generated combining 26 SNIa explosion models in 1D and 3D, including all the explosion mechanisms currently under debate, with different assumptions about the physical state of the ambient medium) with the spectra of well-known remnants, like the Tycho SNR.

The Tycho SNR, which is the best candidate for a Type Ia remnant, has been extensively studied with both *Chandra* and *XMM-Newton*, providing high-quality spectra with precise determinations of the flux and energy centroid of the spectral features produced by each element. One of the main properties of the X-ray spectra of the Tycho remnant is that the emission lines due to Fe and Si (and other intermediate mass elements, like S and Ca) are produced under quite different thermal conditions. Through a careful analysis, Badenes [16] has been able to prove that most of the explosion paradigms are incompatible with the spectra of Tycho. The best approximation to the X-ray spectrum of the Tycho SNR is obtained with a mildly-energetic ($K = 1.2 \times 10^{51}$ erg) 1D (i.e. chemically stratified) delayed detonation model, which synthesizes $0.74 M_{\odot}$ of

^{56}Ni (see Fig. 2). It was shown in this work that, due to the absence of chemical stratification, the SNR models produced by 3D deflagrations and 3D delayed detonations were characterized by the homogeneity of the ionization and thermal properties of all the chemical elements. As we have explained before, such homogeneity is incompatible with the physical properties derived from the X-ray spectra of the Tycho SNR and other candidate Type Ia SNRs. It will be interesting to see whether the spectra predicted by the new 3D explosion paradigms of SNIa will retain these characteristics or, on the contrary, will become more similar to the ones corresponding to 1D explosion models.

SUMMARY

Since Hoyle and Fowler [1] proposed the white dwarf scenario for Type Ia SNe, the ideas about the way the star explodes have evolved. The 70's were the epoch of pure detonations. The 80's witnessed a flourishing of the deflagrations, mainly thanks to the popular W7 model. The 90's knew about delayed detonations in its various flavors. Nowadays, at the beginning of the 21st century, the future of TSN modelling resides most probably on new paradigms, like PRD and GCD.

Although, in the near future, the analysis of Type Ia supernovae will continue being based predominantly on optical observations, the realm of high energies is going to play an increasingly important role in the understanding of these objects. We have discussed some recent progress on the applications of X-ray spectra from young supernova remnants to the determination of the explosion mechanism. Future observations of gamma-rays from SNIa will allow a much more in depth knowledge of the amount of radioactive nuclei produced in the explosion, its distribution throughout the ejecta, and the eventual influence of the interaction with a secondary star in a binary system [see, e.g. 33].

ACKNOWLEDGMENTS

This research has been partially supported by the CIRIT, the MEC programs AYA2002-04094-C03-01/02 and AYA2004-06290-c02-01/02, and by the EU FEDER funds.

REFERENCES

1. Hoyle, F., and Fowler, W., *ApJ*, **132**, 565 (1960).
2. Nugent, P., Baron, E., Branch, D., Fischer, A., and Hauschildt, P., *ApJ*, **485**, 812 (1997).
3. Hillebrandt, W., and Niemeyer, J., *ARA&A*, **38**, 191 (2000).
4. Colgate, S., and McKee, C., *ApJ*, **157**, 623 (1969).
5. Riess, A., Press, W., and Kirshner, R., *ApJ*, **473**, 88 (1996).
6. Hamuy, M., Phillips, M., Suntzeff, N., Schommer, R., Maza, J., and Aviles, R., *AJ*, **112**, 2391 (1996).
7. Perlmutter, S., et al., *ApJ*, **483**, 565 (1997).
8. Phillips, M. M., Lira, P., Suntzeff, N. B., Schommer, R. A., Hamuy, M., and Maza, J., *AJ*, **118**, 1766 (1999).
9. Marion, G. H., Hofflich, P., Vacca, W., and Wheeler, J., *ApJ*, **591**, 316 (2003).

10. Kasen, D., Nugent, P., Wang, L., Howell, D., Wheeler, J., Hofflich, P., Baade, D., Baron, E., and Hauschildt, P., *ApJ*, **593**, 788 (2003).
11. Thomas, R., Kasen, D., Branch, D., and Baron, E., *ApJ*, **567**, 1037 (2002).
12. Thomas, R., Branch, D., Baron, E., Nomoto, K., Li, W., and Filippenko, A., *ApJ*, **601**, 1019 (2004).
13. Li, W., et al., *PASP*, **115**, 453 (2003).
14. Gerardy, C., höflich, P., Fesen, R., Marion, G., Nomoto, K., Quimby, R., Schaefer, B., Wang, L., and Wheeler, J., *ApJ*, **607**, 391 (2004).
15. Hamuy, M., et al., *Nature*, **424**, 651 (2003).
16. Badenes, C., *Thermal X-Ray Emission from Young Type Ia Supernova Remnants*, Ph.D. thesis, Polytechnic University of Catalonia (UPC), Barcelona, Spain (2004).
17. Garcia-Senz, D., and Woosley, S., *ApJ*, **454**, 895 (1995).
18. Woosley, S. E., Wunsch, S., and Kuhlen, M., *ApJ*, **607**, 921 (2004).
19. Garcia-Senz, D., and Bravo, E., *A&A*, **in press** (2004).
20. Reinecke, M., Hillebrandt, W., and Niemeyer, J., *A&A*, **391**, 1167 (2002).
21. Gamezo, V., Khokhlov, A., Oran, E., Chtchelkanova, A., and Rosenberg, R., *Science*, **299**, 77 (2003).
22. Niemeyer, J., Reinecke, M., Travaglio, C., and Hillebrandt, W., “Small Steps Toward Realistic Explosion Models of Type Ia Supernovae,” in [34], p. 151.
23. Garcia-Senz, D., and Bravo, E., “Influence of Geometry on the Delayed Detonation Model of SNIa,” in [34], pp. 158–164.
24. Gamezo, V., Khokhlov, A., and Oran, E., *PhRvL*, **92**, 1102 (2004).
25. Khokhlov, A., *A&A*, **245**, 114 (1991).
26. Woosley, S., and Weaver, T., “Massive Stars, Supernovae, and Nucleosynthesis,” in *Supernovae*, edited by S. Bludman, R. Mochkovitch, and J. Zinn-Justin, Les Houches Session LIV, Elsevier, Amsterdam, 1994, p. 63.
27. Lisewski, A., Hillebrandt, W., and Woosley, S., *ApJ*, **538**, 831 (2000).
28. Plewa, T., Calder, A., and Lamb, D., *ApJ*, **612**, L37 (2004).
29. Badenes, C., Bravo, E., Borkowski, K., and Domínguez, I., *ApJ*, **593**, 358 (2003).
30. Dwarkadas, V., and Chevalier, R., *ApJ*, **497**, 807 (1998).
31. Itoh, H., Masai, K., and Nomoto, K., *ApJ*, **334**, 279 (1988).
32. Kosenko, D., Sorokina, E., Blinnikov, S., and Lundqvist, P., *Advances in Space Research*, **33**, 392–397 (2004).
33. Isern, J., Bravo, E., and Hirschmann, A., *Advances in Space Research*, **in press** (2004).
34. Hillebrandt, W., and Leibundgut, B., editors, *From Twilight to Highlight: The Physics of Supernovae*, Springer, Berlin, 2003.